1   **Hydrothermal Decomposition of Amino Acids and Origins of Prebiotic Meteoritic Organic Compounds**

2

3   Fabio Pietrucci[1], José C. Aponte[2,3,*], Richard Starr[2,4], Andrea Pérez-Villa[1], Jamie E. Elsila[2], Jason P.

4   Dworkin[2], A. Marco Saitta[1,*]

5

6   [1] Sorbonne Université, Muséum National d'Histoire Naturelle, UMR CNRS 7590, IRD, Institut de

7   Minéralogie, de Physique des Matériaux et de Cosmochimie, IMPMC, F-75005, Paris, France

8   [2] The Goddard Center for Astrobiology and Solar System Exploration Division, Code 691, NASA Goddard

9   Space Flight Center, 8800 Greenbelt Road, Greenbelt, Maryland 20771, United States of America

10   [3] Department of Chemistry, The Catholic University of America, 620 Michigan Ave. NE, Washington, DC

11   20064, United States of America

12   [4] Physics Department, The Catholic University of America, 620 Michigan Ave. NE, Washington, DC 20064,

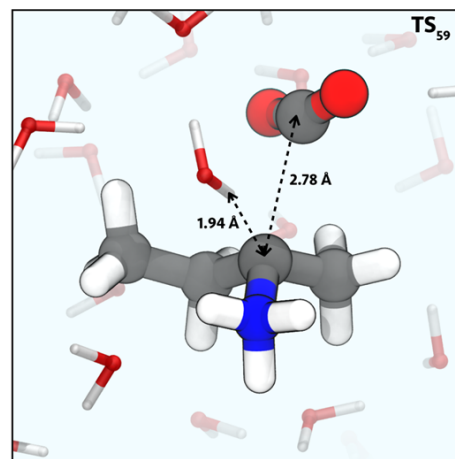13   United States of America

14

15   *** To whom correspondence may be addressed.** Email: jose.c.aponte@nasa.gov (tel.: +1.301.614.6916)

16   or marco.saitta@sorbonne-universite.fr (tel.: +33.01.4427.2244)

17

Table of Contents (TOC) Graphic
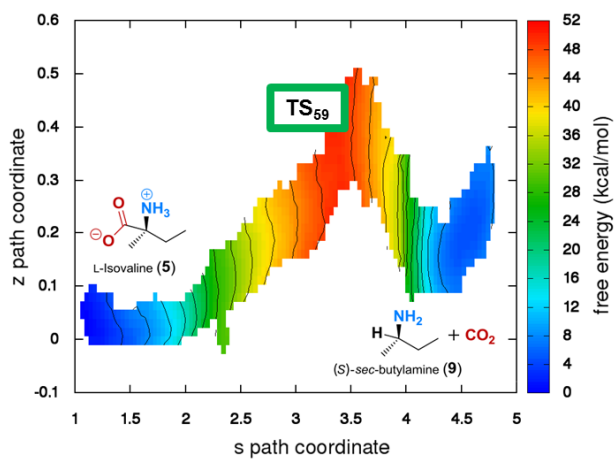
Free-energy landscapes:
Reaction at T = 373 K

Isovaline decarboxylation:
Transition state (TS_{59})

24 **ABSTRACT**

25   The organic compounds found in carbonaceous chondrite meteorites provide insight into
26 primordial solar system chemistry. Evaluating the formation and decomposition mechanisms of
27 meteoritic amino acids may aid our understanding of the origins of life and homochirality on Earth. The
28 amino acid glycine is widespread in meteorites and other extraterrestrial environments; other amino
29 acids, such as isovaline, are found with enantiomeric excesses in some meteorites. The relationship
30 between meteoritic amino acids and other compounds with similar molecular structures, such as aliphatic
31 monoamines and monocarboxylic acids is unclear; experimental results evaluating the decomposition of
32 amino acids have produced inconclusive results about the preferred pathways, reaction intermediates,
33 and if the conditions applied may be compatible with those occurring inside meteoritic parent bodies. In
34 this work, we performed extensive tandem metadynamics, umbrella sampling, and committor analysis to
35 simulate the neutral mild hydrothermal decomposition mechanisms of glycine and isovaline and put them
36 into context for the origins of meteoritic organic compounds. Our *ab initio* simulations aimed to determine
37 free energy profiles and decomposition pathways for glycine and isovaline. We found that under our
38 modeled conditions, methylammonium, glycolic acid, and *sec*-butylamine are the most likely
39 decomposition products. These results suggest that meteoritic aliphatic monocarboxylic acids are not
40 produced from decomposition of meteoritic amino acids. Our results also indicate that the decomposition
41 of L-isovaline prefers an enantioselective pathway resulting in the production of (*S*)-*sec*-butylamine.

INTRODUCTION

Carbonaceous chondrites are natural reaction vessels carrying within their mineral matrix the chemical fingerprint of the early solar system. Their study provides insights into the prebiotic organic synthesis that occurred in the presolar nebula, the protoplanetary disk, and during asteroidal aqueous and thermal processing.[1,2] Meteoritic aliphatic amino acids have been found in representatives of all carbonaceous chondrite groups, have become the most heavily studied organic compounds in meteorites[3-5] because of their contribution to the prebiotic inventory available for the origins of life on Earth. The organic matter accreted and/or synthesized inside asteroids and comets could have been an important source of substrates for the origin and early evolution of life on Earth (and possibly elsewhere). Amino acids can be chiral (exhibit handedness) and only left-handed amino acids (L-enantiomers) are translated in biology (homochirality). In the absence of a chiral driving force, the abiotic synthesis of amino acids results in racemic mixtures (1:1 ratio of L- and D-enantiomers). The transition from racemic abiotic chemistry to homochiral life remains an unanswered key question in origins-of-life research.[6,7] Some meteoritic amino acids possess L-enantiomeric excess, with the best studied example of these being isovaline (e.g., present at up to 18% L-excess[‡] in the Murchison,[8] and other meteorites)[9]. The presence of non-racemic meteoritic amino acids suggests that homochirality on Earth could have been seeded and developed from the delivery of L-enantioenriched amino acids by carbonaceous chondrites.

Low-temperature aqueous alteration of meteoritic parent bodies may have occurred in melting water ices that resulted from heating caused by radioactive decay of short-lived radionuclides and/or by impacts throughout the history of the asteroid parent body.[10-12] These icy inclusions may have contained the starting materials needed for the formation of meteoritic amino acids through the Strecker synthesis, Michael addition, and/or other synthetic routes.[13-15] Aqueous processes in the parent body of the Murchison and other carbonaceous chondrites belonging to varying petrologic types have been proposed to occur at pH ranging from 6-12,[16] however, this value may greatly depend on the temperature of the system, adsorption of ions, flows of gases and fluids, and the specific mineral composition of the sample, among other parameters.[17] Additionally, continuous heating of these aqueous inclusions may have

---

[‡] (*S*)- and (*R*)-notations are more appropriate, however, the amino acid literature uses L- and D-notations based on analogy with glyceraldehyde; for consistency to the nomenclature used in previous meteoritic amino acid studies, we equate (*S*)- to L- and (*R*)- to D- based on their structures.

69   resulted in the decomposition of synthesized amino acids through interactions with liquid water and

70   mineral.[18-20] It has been suggested that the decomposition of amino acids through deamination and

71   decarboxylation driven by aqueous and thermal processes inside the asteroid parent body may result in

72   the formation of carboxylic acids and amines.[21-23] Both aliphatic carboxylic acids and amines have been

73   isolated from carbonaceous chondrites.[21-26] To date, however, the role of amino acids in the production

74   of carboxylic acids and amines through their decomposition under asteroid-like conditions remains poorly

75   understood.[27]

76   In this work, we modeled the effects of asteroidal aqueous processing on the decomposition of

77   amino acids leading to the formation of monocarboxylic acids and monoamines (hereafter called

78   "carboxylic acids" and "amines"). We selected the amino acids glycine and isovaline as proxies for studies

79   of amino acid decomposition under meteoritic conditions using full atomistic molecular dynamics (MD)

80   simulations based on density functional theory (DFT). Glycine is a common achiral amino acid which has

81   been identified in all carbonaceous chondrites and in other extraterrestrial environments, including lunar

82   regolith and comets.[28-31] The chiral amino acid isovaline is rare in the terrestrial biosphere but common in

83   many carbonaceous chondrites and is of interest because excesses of its L-enantiomer have been

84   measured in several meteorites,[8,9,32-34] creating a potential link between its exogenous delivery to Earth

85   and the origins of terrestrial biological homochirality. Our computational study aimed to unveil

86   prospective synthetic relationships between meteoritic amino acids, carboxylic acids, and amines and the

87   maturation of meteoritic organics prior to, during, and after their formation in the asteroid parent body.

88   The key component of this work was assessing the decomposition mechanisms of amino acids in

89   hydrothermal aqueous solution and identifying their decomposition products to establish potential links

90   for the origins of some meteoritic soluble organic compounds. Experimental results on the decomposition

91   of amino acids often produce controversial and, in some cases, contradictory results,[35] leaving unclear

92   whether amino acids would preferentially decompose through decarboxylation or deamination and what

93   the identity of their reaction intermediates are under neutral hydrothermal conditions that may be

94   compatible with those experienced inside the asteroid parent body. Our recently developed approach,

95   which defines a class of general topological reaction coordinates, is particularly well suited for complex

96   multistep mechanisms in aqueous media.[36] We performed *ab initio* molecular dynamics simulations

97   (Born-Oppenheimer) combined with advanced techniques for enhanced sampling of rare events and the

98   reconstruction of free energy landscapes and kinetics (metadynamics, umbrella sampling, weighted

99   histogram analysis, committor analysis)[37-38]. Our simulation clarifies the decomposition products and

100 synthetic origins of prebiotic molecules in meteorites related to glycine and isovaline, shedding new light

101 on fundamental atomic-level mechanisms behind meteoritic prebiotic chemistry.

102 **METHODS**

103 *Ab initio* **molecular dynamics and free energy calculations**

104   We explored the decomposition products of glycine and isovaline using *ab initio* MD, which has

105 well demonstrated its predictive power in describing amino acid synthesis in computer simulations of the

106 Miller experiments.[39] The asteroidal conditions were constrained based on previous meteoritic petrologic

107 analyses, which suggest that aqueous alteration occurred between 0 and 340 °C).[16,40-43] Amino acids may

108 be present as neutral zwitterions inside the parent body based on large abundances of ionic species

109 (cation and anions from mineral complexes and water-soluble salts). To model asteroid-like hydrothermal

110 processing, we selected a temperature of 100 °C and an aqueous environment in which amino acids would

111 be present as zwitterions. We acknowledge that the conditions for hydrothermal processing situates the

112 reactions in bulk water, without explicit consideration of minerals and the presence of species such as a

113 CO_2, CO, and ammonia commonly found in meteorites;[24,44] however, the chosen conditions provide

114 fundamental information on amino acid reaction pathways that may serve as a reference for future

115 experimental and computational works focusing on, for example, the specific effects of particular mineral

116 surfaces on amino acid decomposition.

117   Born-Oppenheimer MD simulations (at T = 373 K) were performed using interatomic forces

118 computed at DFT level (Perdew-Burke-Ernzerhof functional with Grimme's van-der-Waals

119 corrections).[45,46] Kohn-Sham valence wave functions were expanded on a plane wave basis, as

120 implemented in the CPMD code[47] optimally designed for massively parallel computers. Free energy

121 landscapes were reconstructed employing in tandem metadynamics[48] and umbrella sampling;[49] the

122 former for a fast discovery of reaction pathways and preliminary estimation of barriers, and the latter for

123 a precise sampling of selected pathways. A key component of our approach are path collective variables

124 based on coordination patterns,[38] that allow us to discover unforeseen reaction mechanisms and to obtain

125 reversible pathways without human prejudice about transition states or intermediates. The model

126 consisted of a periodically repeated box including one amino acid molecule (glycine or isovaline) solvated

127 with 79 water molecules. Our simulations followed protocols similar to those previously published,[40] and

128 exploited the plugin Plumed;[50] further details are provided in Supplementary Information. We cannot

129 exclude the existence of amino acid decomposition pathways different from those described in the

130 following sections. However, the reaction mechanisms characterized in this work are the result of

131 extensive *ab initio* simulations, totaling more than 3 ns (80 ps of equilibration trajectories, 300 ps of

132 exploratory metadynamics, 2000 ps of umbrella sampling, and 1000 ps of committor analysis), equivalent

133   to 1.3 million Intel® Xeon® E5-2690v3 hours. For comparison, the majority of published *ab initio* molecular

134   dynamics studies of chemical reactivity are limited to a total simulation length of tens of ps.

135   **RESULTS**

136   **Decomposition of amino acids**

137   Glycine and isovaline differ at the alpha-carbon (C_α; Scheme. 1), leading to significant differences

138   in their decomposition pathways; in glycine, the C_α is accessible to the solvent, whereas in isovaline the

139   C_α is protected by a coordination shell of four heavy atoms. We investigated the decomposition of glycine

140   and isovaline through deamination or decarboxylation pathways in simulated asteroidal hydrothermal

141   processing under aqueous neutral conditions, the investigated mechanisms are shown in Figure 1 panels

142   a and b. Additionally, we show the schematic summaries of the step-by-step reaction mechanisms for

143   glycine and isovaline decompositions in Figures S1, S2, and Movies S1-S6 available in the Supplementary

144   Information. Corresponding free energy profiles and landscapes are shown in Figure 2 and Figure 3

145   respectively, and representative transition state and electronic structures are depicted in Figures 4 and 5.

146   The two decomposition mechanisms of solvated glycine (**1**) and isovaline (**5**) start from their

147   favored zwitterionic species (Figure 1). The deamination of glycine does not show the formation of acetate

148   (**2′**), which is the simplest aliphatic deamination product one could envisage; indeed, the loss of neutral

149   ammonia from the glycine zwitterion would leave a carbocation species that, formally, would need the

150   addition of a hydride (H^-) to form acetate. Note, however, that this reaction is not viable in practice: even

151   if a hydride were present in solution, it would probably undergo a different fate (reduction of the glycine

152   carboxylate group; reaction not shown here). Instead, the deamination of glycine results in two possible

153   end products: neutral glycolic acid (**2**) and ammonia, or their conjugate base/acid glycolate (**3**) ammonium

154   salt (Figure 1A). The free energy landscape reveals an identical barrier of 40 kcal/mol for these two

155   deamination results (Figures 2a, 3a, 3b, and Table S1 which shows a summary of the simulated reactions

156   free energy barriers in kcal/mol). However, the two possible end states have different stabilities, with the

157   charged species being lower in free energy by 5 kcal/mol, as expected from the pK_a of glycolic acid (3.83

158   at 300 K) and from the pK_b of ammonia (4.7). The configuration of the transition state was identified by

159   committor analysis, and a representative structure is shown in Figure 4a. The transition state is

160   characterized by the partial breaking of the C–N bond with simultaneous splitting of a water molecule and

161   hydroxide (OH^-) nucleophilic attack at the C_α (with partial carbocation character; Figures 4a and 5a).

162   The free energy landscape for glycine decarboxylation is depicted in Figure 3c. The transition state

163   (Figures 4b and 5b) is characterized by the simultaneous i) partial breaking of the C–C bond, ii) partial

164   linearization of the CO_2 group, and iii) a half-split water molecule, whose proton moves towards the

165   C_α atom (with partial carbanion character). We estimated a free energy barrier of 43 kcal/mol, very similar

9

166   to that found for deamination. The product state appears 12 kcal/mol less stable than reactants; however,

167   we note that the further reaction [CO_2 + OH^- → HCO_3^-] is expected to decrease the free energy by 10

168   kcal/mol,[51] bringing glycine to a similar stability with respect to [$CH_3NH_3^+$ + HCO_3^-] (Figure 2a, Table S1).

169   Compared to glycine, isovaline (**5**) displays a similar decarboxylation pathway, leading to the

170   formation of *sec*-butylamine (**9**), but a different deamination pathway resulting in products (**6** and **7**)

171   which in turn may decarboxylate to yield 2-butene (**8**; Figures 1b and 2b). Similar to the deamination of

172   glycine, no presence of the unsaturated deaminated analog, 2-methyl butanoate (**7'**) was observed as a

173   deamination product of isovaline (the same argument observed above for glycine can be invoked here).

174   The deamination of isovaline yields two products as the possible outcomes of the same transition state,

175   corresponding to a barrier of 36 kcal/mol (Figures 2b, 3d, 4c, 5c). The first product is 2,2-ethyl-methyl-α-

176   acetolactone (**6**) (albeit with a C–O–C bridge that is intermittently formed and broken on the picosecond

177   time scale), structurally simple to reach from the transition state by reducing the C–C–O angle. This species

178   is, however, quite unstable, with a free energy 32 kcal/mol higher than isovaline (Figures 2b, 3d). A more

179   stable product, lying at 20 kcal/mol above isovaline, is *cis*-2-methyl-2-butenoic acid (commonly known as

180   angelic acid, **7**) in its carboxylate anionic form, obtained after deprotonation (operated by the leaving

181   ammonia molecule) of the methylene group with concomitant formation of a C=C double bond. We

182   remark that a single transition state (labeled $TS_{5(6,7)}$ in Figures 2-5) leads to compounds **5**, **6**, **7** with equal

183   probability, as we explicitly tested with committor analysis. Note that the *trans* isomer of **7**, known as

184   tiglic acid, could also be obtained by a similar mechanism, however we did not explicitly perform the latter

185   simulation. Experimentally, pure angelic acid tends to irreversibly convert to tiglic acid, which is more

186   stable by 8.5 kcal/mol than angelic acid as deduced by heats of combustion.[52] Therefore, at 100 °C, our

187   simulations suggest that an isovaline decomposition to angelic/tiglic acid will result in an equilibrium ratio

188   of about 10^{-7} between products and reactants.

189   We extended our metadynamics simulations to explore possible further evolution of angelic acid

190   (**7**) toward decarboxylation, by explicitly targeting this reaction with extensive umbrella sampling

191   simulations. Starting from **7**, a barrier of 55 kcal/mol leads to the cleavage of the C–COO^- bond and

192   protonation of the C_α from a water molecule, eventually resulting in the formation of carbon dioxide and

193   2-butene (Figures 2b and 3e,). The high barrier may be explained by the relative inaccessibility of the C_α

194   to solvent molecules, due to surrounding bulky groups, until a significant elongation of the C–COO^- bond

195   is achieved (Figures 4d and 5d). We remark that if, instead, decarboxylation is attempted starting from

196   2,2-ethyl-methyl-α-acetolactone (**6**), the system rapidly evolves first into angelic acid, confirming that this

197   lactone is an unlikely deviation, apparently of scarce relevance in the reconstructed reaction network. Our

198   results suggest that decarboxylation of angelic acid entails a very large free energy barrier, and results in

199   products of very low stability compared to isovaline; thus, it is not expected that 2-butene derived from

200   isovaline would significantly contribute to the observed pool of meteoritic organic molecules.

201   Direct isovaline decarboxylation proceeds through a simple mechanism (Figure 1), yielding *sec*-

202   butylamine after crossing a barrier of 48 kcal/mol (Figures 2b, Table S1). This decomposition channel is

203   potentially relevant: compared to deamination, decarboxylation encompasses a much higher barrier (with

204   half-life of 10^7 years at 100 °C or 10^4 years at 150 °C, as estimated from Eyring's transition state theory

205   formula) but, in turn, it leads to a much more stable product (only 2 kcal/mol above isovaline; Figures 2b

206   and 3f). Similar to the reaction connecting angelic acid (**7**) with 2-butene, the mechanism involves the

207   cleavage of the C–COO⁻ bond and the protonation of the C_α atom from a water molecule (Figures 4e and

208   5e). At the transition state, the C_α keeps a tetrahedral sp^3 character, enabling access to solvent only on

209   the same side as the leaving CO_2 moiety and protecting the opposite side by steric hindrance. This is

210   confirmed by inspection of all the available trajectories in the transition state region, including umbrella

211   sampling and committor analysis. Thus, the solvent proton replaces the carboxylate functional group

212   without changing the chirality of the C_α. We conclude that the decarboxylation pathway itself does not

213   lead to *sec*-butylamine racemization. We note, instead, that the presence of the α-hydrogen on *sec*-

214   butylamine is generally accepted to strongly increase its hydrothermal racemization rate. In our specific

215   case, this indicates that *sec*-butylamine derived from isovaline would racemize at a faster rate than its

216   parent amino acid inside the asteroid parent body. Preliminary metadynamics simulations suggested

217   other possible decarboxylation mechanisms, such as simultaneous isovaline decarboxylation and

218   deamination, or the formation of formic acid instead of carbon dioxide; however, such pathways turned

219   out to be unlikely under the scrutiny of umbrella sampling.

220   **DISCUSSION**

221   **Comparison to previous computational modeling and experimental results**

222   The current understanding of amino acid decomposition processes in solution is mostly based on

223   experimental information. The most relevant theoretical study to date addressed glycine and alanine

224   decomposition based on a quantum mechanics / molecular mechanics (QM/MM) approach, with the

225   amino acid and up to two water molecules described with a semi-empirical molecular orbital method ,

226   immersed in a bath of classical water molecules.[53] The previous work yielded a glycine decarboxylation

227   barrier of 46 kcal/mol, close to ours. In our simulations, based on a more accurate quantum description

228   and on more general collective variables, we find that, with respect to the previous work, the products

229   are significantly less stable than the reactants. Concerning glycine deamination, Alexandrova and

230   Jorgensen (2011) reported a free energy barrier of 51 kcal/mol for the formation of an α-lactone, and >

231   90 kcal/mol for the formation of glycolic acid. Instead, we predict glycolic acid formation as the only viable

232   reaction, with a much lower barrier of only 40 kcal/mol, in good agreement with experiments as discussed

233   below, thus pointing to a more accurate description of the reaction pathway in our framework.

234   The interpretation of the available experimental results in the literature is controversial. As

235   pointed out by Cox and Seward (2007), various reports using different experimental conditions and

236   reaction vessels often presented contradictory conclusions, so that it is not clear whether glycine and

237   other amino acids preferentially decarboxylate or deaminate, and through which mechanism. In several

238   cases, decarboxylation was *a priori* assumed to happen, and deamination was not explicitly tested. A

239   decarboxylation enthalpy barrier of 39 kcal/mol above 170 °C was inferred from NMR analyses,[54] and

240   similarly from chromatography above 200 °C.[51] Snider and Wolfenden (2000) also reported a slow-down

241   of the reaction with increasing ionic strength, suggestive of a transition state less polarized than the

242   reactants, which is consistent with the decomposition mechanisms found in this work. An enthalpy barrier

243   of 33 kcal/mol was inferred from an *in situ* infrared spectrometer flow reactor above 310 °C.[56] The free

244   energy barriers we observed for deamination and decarboxylation are similar within statistical errors

245   (about 2 kcal/mol), and using Eyring formula ($k = k_B T/h \ e^{-\Delta G^*/k_B T}$) the corresponding decomposition rate is

246   between 10^{-11} and $10^{-13} \, s^{-1}$ at 100 °C, equivalent to half-lives between one thousand and several tens of

247   thousands of years; the upper rate is in agreement with experimental measurements.[54-56] Given the

248   survival of amino acids in meteorites to the present day, these half-lives would be consistent with

249   suggestions that although there may have been available liquid water for several millions of years inside

250   the parent body, the alteration processes may have only been episodic and not continuous throughout

12

251 that period of time (i.e. episodes of aqueous alteration may have been triggered by short-term events like

252 impacts).[42]

253 Similar to chromatographic experiments,[55] and based on our findings, we conclude that

254 deamination and decarboxylation decomposition pathways could be simultaneously available in a

255 hydrothermal glycine solution. The simulations, however, predict the formation of ammonium glycolate

256 and methylammonium bicarbonate ions at a similar pace, with the latter products being much more stable

257 than the former (if the exothermic hydroxylation of CO_2 occurs starting from methylammonium) and in

258 similar equilibrium proportions as the glycine reactants. From the kinetic point of view, deamination

259 appears to be moderately favored over decarboxylation, even if the free energy difference of 3 kcal/mol

260 does not appear very significant considering statistical uncertainties as well as the intrinsic accuracy of

261 DFT calculations.[57] Therefore, following long-term aqueous conditions on asteroid parent bodies,

262 methylamine is expected as the dominant meteoritic glycine decomposition product (leaving aside the

263 possibility of products themselves entering further reaction pathways). Indeed, the abundance of amines

264 is greater than that of amino acids in meteorites experiencing extended increasing aqueous processing,

265 while the opposite is true in minimally aqueously altered carbonaceous chondrites.[23-26] It should be noted

266 that *in situ* spectrophotometric measurements pointed to sizable glycine dimerization in addition to

267 decomposition.[35] However, investigating such additional multi-molecular process is beyond the scope of

268 this work.

269

270 **Constraints of our asteroid-like processing model**

271 Our work provides detailed quantitative insight about amino acid decomposition reactions in

272 simulated asteroidal hydrothermal conditions; however, discussions of the interpretation and relevance

273 of these results from the point of view of asteroid parent body processes and meteorite organics must

274 consider the following factors. First, we chose a specific temperature and two amino acids particularly

275 representative of meteoritic chemistry: the simplest and most common one (glycine), and the one with

276 the most reports of L-enantiomeric excess in meteorites (isovaline). Temperatures above 100 °C and a

277 higher concentration of protons or catalytic transition metal ions, which may have occurred for

278 extensively altered chondrites, may strongly alter the amino acid decomposition kinetics. Second, the

279 reaction network we reconstructed (Figure 1) is part of a larger scheme in which amino acid

280 decomposition products can take part in further reactions with other species not explicitly considered

281 here. In this sense, even a relatively evanescent intermediate, of apparent low relevance, could increase

282   the available molecular inventory, and possibly play a key role toward a stable product in the more global

283   prebiotic network in the parent body. Third, the reaction rates and equilibrium populations we inferred

284   are pertinent to bulk, neutral water solutions. As such, they provide a reference reaction network that

285   can be used as a starting point to address various questions about the viability of different prebiotic

286   scenarios, including: what is the optimal range of temperature for a given reaction?; would an acidic or

287   alkaline pH favor a synthetic/decomposing pathway?; under what conditions would mineral surfaces play

288   significant role in stabilizing transition states, intermediates, and products? These are questions that

289   future experimental and theoretical efforts may be able to answer, incrementing our understanding about

290   the origins of prebiotic meteoritic organic matter.

291

Implications for the origins of some meteoritic soluble organic compounds

293   Although meteoritic organic compounds formed in distinct stages through the birth and

294   evolution of the solar system, we can constrain their origin to two main environments and regimes: (1)

295   pre-parent body, dominated by gas- and ice-grain chemistry that occurred in the molecular cloud, the

296   solar nebula, or the protoplanetary disk, and (2) parent body, dominated by hydrothermal processes.

297   Given the unknown concentration of the molecular species available for chemical development, the

298   unsettled and changing physical conditions such as temperature and pressure, and the uncertain level of

299   processing that occurred in each parent body, it may prove challenging to assess the dominant synthetic

300   routes leading to the origins of meteoritic amino acids.[27] However, it is useful to note that (a) the detection

301   of the simplest amino acid (glycine) in the interstellar medium remains controversial,[58,59] (b) the observed

302   abundances of meteoritic amino acids and those synthesized after hydrolysis of UV-irradiated interstellar

303   ice analogs decreases with increasing carbon,[60,61] and (c) only aminoacetonitrile, but no glycine, has been

304   observed before the hydrolysis of interstellar ice analogs irradiated at temperatures ranging from 20 to

305   300 K.[62] From these observations, it can be suggested that some degree of processing inside the parent

306   body may favor augmenting the molecular abundance and diversity of meteoritic amino acids, and that

307   prolonged processing could result in the amino acid decomposition pathways studied here.

308   From our computational analyses, we have found that the deamination and decarboxylation of

309   glycine occurs with similar barriers leading to the production of the hydroxylated acid (glycolic acid) and

310   methylamine. In contrast, the deamination and decarboxylation of isovaline occurs at different rates, and

311   it is not the hydroxylated acid, but rather the α-β-unsaturated acid (**7**) that would be the fastest

312   decomposition product over *sec*-butylamine, although the amine is expected to dominate at equilibrium

313   by virtue of its higher stability. The difference in decomposition products may originate from the relative

314   inaccessibility of the C_α to solvent molecules in isovaline relative to glycine (see Scheme 1 and electron

315   localization function – ELF - analysis shown in Figure 5). It should be noted, furthermore, that neither the

316   decarboxylation of glycine nor that of isovaline result in the formation of formic acid. This observation

317   suggests that meteoritic formic acid must have formed before the accretion of the parent body, or through

318   reaction mechanisms that are not related to the decomposition of amino acids inside the parent body,

319   e.g., catalytic hydrogenation of CO_2, or the hydrolysis of the methyl formate produced by the reaction of

320   methanol and carbon monoxide.

321   Our results do not provide evidence for the formation of saturated aliphatic monocarboxylic

322   acids, namely, acetic acid and 2-methylbutanoic acid, as deamination products of glycine and isovaline

323   respectively. These carboxylic acids have been detected in various carbonaceous chondrites and

324   constitute some of the most abundant water-soluble organic compounds in meteorites,[22,24,25,63] but our

325   calculations suggest that deamination of amino acids does not contribute to their reported abundances.

326   This contrasts with methylamine and *sec*-butylamine, the corresponding decarboxylation products of

327   glycine and isovaline. This observation suggests that either aliphatic acids originated in cold interstellar

328   pre-solar regions and were later incorporated inside the parent body, or that they formed from organic

329   species that underwent synthetic processes other than glycine and isovaline decomposition, e.g.,

330   oxidation of aliphatic aldehydes or hydrolysis of alkyl nitriles inside the parent body.

331   Our calculations show an α-β-unsaturated compound (angelic acid, **7**) as the deamination product

332   of isovaline, with a further decarboxylation leading to 2-butene. The abundance of **7** (or any other α-β-

333   unsaturated monocarboxylic acid) has not been evaluated in analyses of meteoritic organics. Although 2-

334   butene has been reported in analyses of extracts from the Murchison meteorite in a mix of isomers,[24] this

335   decomposition pathway exhibits a very high barrier that suggests that the meteoritic origins of 2-butene

336   would not be necessarily related to the decomposition of the amino acid, except in cases of extended

337   hydrothermal processing at higher temperatures. Another possibility is that **7** could react to form β-amino

338   acids inside the parent body, considering that α-β-unsaturated carboxylic species readily undergo 1,4-

339   nucleophilic additions.[64-65] Indeed, the concentration of β-amino acids is higher than that of α-amino acids

340   in more extensively aqueously altered carbonaceous chondrites.[34,66] Our computational results of the

341   deamination of isovaline (an α-alkyl-α-amino acid) would support a parent body scenario in which the

342   concentration of β-amino acids increases at the expense of the decomposition of α-amino acids through

15

343   aqueous alteration. However, the possibility that the higher abundance of β-amino acids may be an
344   inherent characteristic of the parent body's molecular budget might not be discarded.

345   The more stable decarboxylation product of isovaline, *sec*-butylamine, has been found in
346   carbonaceous chondrites exhibiting varying levels of aqueous and thermal processing.[28,67] The stability of
347   *sec*-butylamine is consistent with the idea that at least a portion of this meteoritic amine may be produced
348   upon decomposition of the amino acid either in the parent body stage or through amino acid extraction
349   (the extraction of amino acids from meteoritic samples is typically done using hot water at 100 °C) and
350   sample processing during analyses.

351   In addition to the detailed decomposition pathways shown here and reading the reactions in
352   Figure 1 in reverse order, it can be predicted that glycine could be obtained from methylamine or from
353   glycolic acid, and isovaline from *sec*-butylamine or from angelic acid, through relatively-low free energy
354   barriers that range from 15 to 45 kcal/mol. These results suggest that the synthesis of meteoritic amino
355   acids under hydrothermal conditions appear feasible even without invoking the aid of catalyzers or
356   synthetic routes such as the Strecker-cyanohydrin synthesis, similar to recent experimental results.[15] Our
357   predictions could be tested in future experiments, helping to inform both terrestrial and extraterrestrial
358   amino acid formation processes.

359

360   **Enantiomeric excess at the dawn of the solar system**

361   The enantiomeric excess (*ee*) of L-isovaline has been observed in meteorites with various
362   processing histories,[8,9,33,34] and a direct relationship has been suggested between the degree of aqueous
363   alteration and the percentage of L-*ee* found in carbonaceous chondrites.[8] The enantiomeric composition
364   of meteoritic *sec*-butylamine has shown contradictory results. Aponte et al. (2015, 2016), reported
365   racemic mixtures of *sec*-butylamine in carbonaceous chondrites from which enantiomeric excesses of L-
366   isovaline was found ranging from 0 to 18%. In contrast, enantiomeric enrichments of (*S*)-*sec*-butylamine
367   ranging from 0 to 66% in moderately and minimally aqueously altered CR2 and CR3 chondrites in which
368   isovaline was racemic (L-*ee* from 0 to 3 ± 4%[34,68]) was also reported.[69] One notable piece of information
369   obtained from our models is the enantioselective decomposition of isovaline into *sec*-butylamine.
370   According to this result, any *ee* present in L-isovaline, would be conserved when decarboxylated into (*S*)-
371   *sec*-butylamine, indicating that an observed (*S*)-*ee* of *sec*-butylamine could be a potential indicator of L-
372   isovaline *ee*. Additionally, our results suggest that *sec*-butylamine will racemize at a faster rate than

373 isovaline given the presence of the α-hydrogen and the lower steric hindrance; in fact, isovaline is more

374 stable against racemization relative to α-H-α-amino acids.[70]

375   The lack of observed *ee* of *sec*-butylamine in meteorites across varying degrees of alteration and

376 in meteorites with a significant L-isovaline *ee* may suggest that, despite our theoretical results, the

377 decarboxylation of enantioenriched isovaline is not a major reaction in the parent body. However,

378 alternate explanations exist, including that: (a) enantioenriched *sec*-butylamine is not observed because

379 of the expected faster racemization of the amine relative to that of isovaline, or (b) a small L-*ee* of isovaline

380 existed that created an *ee* in *sec*-butylamine formed upon decomposition that is below current detection

381 limits, but that parent-body conditions subsequently amplified the isovaline *ee*,[71,72] without having a

382 significant effect on the enantiomeric composition of *sec*-butylamine. The (*S*)-*sec*-butylamine *ee* reported

383 by Pizzarello and Yarnes (2016) would suggest that *sec*-butylamine and isovaline may be synthetically

384 linked through the decomposition of the amino acid in those less-aqueously-altered carbonaceous

385 chondrites.

386   **CONCLUSIONS**

387   In this work, we modeled the effects of aqueous processing leading to the decomposition of the
388   amino acids glycine and isovaline through deamination and decarboxylation. We have been mindful of
389   not being contradicting or confusing towards the broader scientific community in our mechanistic
390   assessments. Our work aimed to be a stepping point for future work that may link computational and
391   experimental analyses to the origins of organic matter in the solar system; no changes were made to the
392   text. Our results have several implications for the origins of soluble meteoritic organic compounds such
393   as amino acids, carboxylic acids and amines. We found that the deamination and decarboxylation of
394   glycine occur through similar barriers, suggesting that both processes would occur in parallel inside the
395   parent body. In contrast, we found that the deamination of isovaline occurs at a faster rate than
396   decarboxylation, and that this process results in the formation of an α-β-unsaturated acid. This may help
397   to explain the observed increase in relative abundance of β-amino acids compared to α-amino acids in
398   meteorites with increasing levels of aqueous processing. Additionally, although aliphatic amines were
399   found as decarboxylation products of glycine and isovaline, our computations did not find evidence for
400   the formation of analogous aliphatic carboxylic acids after deamination, suggesting that these compounds
401   may have synthetic origins that are not related to the decomposition of amino acids inside the parent
402   body. Finally, we found that the decarboxylation of isovaline occurs in an enantioselective fashion,
403   meaning that the chiral configuration of isovaline would be conserved in the *sec*-butylamine produced.
404   The decomposition of isovaline in meteorites exhibiting L-*ee* of this amino acid would produce (*S*)-
405   enantioenriched *sec*-butylamine, although the enantioenriched amine could then racemize more quickly
406   than its amino acid precursor.

Acknowledgments

417   **References**

418   (1)   Cronin J. R.; and Chang S. (1993) Organic matter in meteorites: molecular and isotopic analyses of
419   the Murchison meteorite. In *The Chemistry of Life's Origins* (eds. J. M. Greenberg, C. X. Mendoza-
420   Gómez and V. Pirronello), pp. 209-258. Kluwer Academic Publishers.

421   (2)   Pizzarello S.; Cooper G. W.; and Flynn G. J. (2006) The nature and distribution of the organic material
422   in carbonaceous chondrites and interplanetary dust particles. In *Meteorites and the Early Solar*
423   *System II* (eds. D. S. Lauretta and H. Y. McSween), pp 625-651. University of Arizona Press: Tucson,
424   AZ.

425   (3)   Burton, A. S.; Stern, J. C.; Elsila, J. E.; Glavin, D. P.; Dworkin, J. P. Understanding prebiotic chemistry
426   through the analysis of extraterrestrial amino acids and nucleobases in meteorites. *Chem. Soc. Rev.*
427   **2012**, *41*, 5459-5472.

428   (4)   Cobb, A. K.; Pudritz, R. E. Nature's starships. I. Observed abundances and relative frequencies of
429   amino acids in meteorites. *Astrophys. J.* **2014**, *783*, 140 (12pp).

430   (5)   Elsila, J. E.; Aponte, J. C.; Blackmond, D. G.; Burton, A. S.; Dworkin, J. P.; Glavin, D. P. Meteoritic
431   amino acids: Diversity in compositions reflects parent body histories. *ACS Cent. Sci.* **2016a**, *2***,** 370-
432   379.

433   (6)   Dragos Gherase, Robert M. Hazen, Ramanarayanan Krishnamurthy, Donna G. Blackmond. Mineral-
434   Induced Enantioenrichment of Tartaric Acid. Synlett 2017; 28(01): 89-92.

435   (7)   Alexander J. Wagner, Dmitry Yu. Zubarev, Alán Aspuru-Guzik, and Donna G. Blackmond. Chiral
436   Sugars Drive Enantioenrichment in Prebiotic Amino Acid Synthesis. ACS Cent. Sci. 2017, 3, 322–328.

437   (8)   Glavin D. P., and Dworkin J. P. (2009) Enrichment of the amino acid L-isovaline by aqueous alteration
438   on CI and CM meteorite parent bodies. Proceedings of the National Academy of Sciences **106**, 5487-
439   5492.

440   (9)   Burton A. S., Elsila J. E., Hein J. E., Glavin D. P. and Dworkin J. P. (2013) Extraterrestrial amino acids
441   identified in metal-rich CH and CB carbonaceous chondrites from Antarctica. *Meteorit. Planet. Sci.*
442   **48**, 390-402.

443   (10)   Grimm R. E., and McSween H. Y. Jr. (1989) Water and the thermal evolution of carbonaceous
444   chondrite parent bodies. Icarus **82**, 244-280.

445   (11)   Shukolyukov A., Lugmair G. W. (1993) Fe-60 in eucrites. Earth and Planetary Science Letters **119**,
446   159-166.

447   (12)   Rosenberg N. D. et al. (2001) Modeling aqueous alteration of CM carbonaceous chondrites. Meteor.
448   Planet. Sci. **36**, 239-244.

449   (13) Peltzer E. T., Bada J. L., Schlesinger G. and Miller S. L. (1984) The chemical conditions on the parent

450   body of the Murchison meteorite: some conclusions based on amino, hydroxy and dicarboxylic

451   acids. Adv. Space Res. **4**, 69-74.

452   (14) Cooper, G. & Cronin, J. R. Linear and cyclic aliphatic carboxamides of the Murchison meteorite:

453   Hydrolyzable derivatives of amino acids and other carboxylic acids. Geochim. Cosmochim. Acta **59**,

454   1003–1015 (1995).

455   (15) Koga and Naraoka (2017) A new family of extraterrestrial amino acids in the Murchison meteorite.

456   Scientific Reports **7**, 636.

457   (16) Zolensky, M.E., Bourcier, W.L., Gooding, J.L., 1989. Aqueous alteration on the hydrous asteroids:

458   Results of EQ3/6 computer simulations. Icarus **78**, 411-425.

459   (17) Zolotov M. Y. (2012) Aqueous fluid composition in CI chondritic materials: Chemical equilibrium

460   assessments in closed systems. Icarus **220**, 713-729.

461   (18) Rodante, F., Thermodynamics and kinetics of decomposition processes for standard α-amino acids

462   and some of their dipeptides in the solid state. Thermochim. Acta 1992, **200**, 47-61.

463   (19) Cohen B. A., and Coker R. F. (2000) Modeling of Liquid Water on CM Meteorite Parent Bodies and

464   Implications for Amino Acid Racemization. Icarus **145**, 369-381.

465   (20) Kebukawa Y., Chan Q. H. S., Tachibana S., Kobayashi K., Zolensky M. E. (2017) One-pot synthesis of

466   amino acid precursors with insoluble organic matter in planetesimals with aqueous activity. Science

467   Advances **3**: e1602093.

468   (21) Pizzarello S., Feng X., Epstein S., and Cronin J. R. (1994) Isotopic analyses of nitrogenous compounds

469   from the Murchison meteorite: ammonia, amines, amino acids, and polar hydrocarbons. Geochim.

470   Cosmochim. Acta **58**, 5579-5587.

471   (22) Aponte J. C., Alexandre M. R., Wang Y., Brearley A. J., Alexander C. O'D., and Huang Y. (2011) Effects

472   of secondary alteration on the composition of free and IOM-derived monocarboxylic acids in

473   carbonaceous chondrites. Geomchim. Cosmochim. Acta **75**, 2309-2323.

474   (23) Aponte J. C., Dworkin J. P., and Elsila J. E. (2015) Indigenous aliphatic amines in the aqueously altered

475   Orgueil meteorite. Meteoritics & Planetary Science **50**, 1733-1749.

476   (24) Yuen G., Blair N., Des Marais D. J., and Chang S. (1984) Carbon isotopic composition of individual,

477   low molecular weight hydrocarbons and monocarboxylic acids from the Murchison meteorite.

478   Nature **307**, 252-254.

479   (25) Huang Y., Wang Y., Alexandre M. R., Lee T., Rose-Petruck C., Fuller M. and Pizzarello S. (2005)
480   Molecular and compound-specific isotopic characterization of monocarboxylic acids in
481   carbonaceous meteorites. Geochim. Cosmochim. Acta **69**, 1073-1084.

482   (26) Aponte J. C., McLain H. L., Dworkin J. P., and Elsila J. E. (2016) Aliphatic amines in Antarctic CR2, CM2
483   and CM1/2 carbonaceous chondrites. Geomchim. Cosmochim. Acta **189**, 296-311.

484   (27) Aponte J. C., Elsila J. E., Glavin D. P., Milam S. N., Charnley S. B., Dworkin J. P. 2017. Pathways to
485   meteoritic glycine and methylamine. ACS Earth & Space Chemistry **1**, 3-13.

486   (28) Glavin, D. P.; Dworkin, J. P.; Sandford, S. A. Detection of cometary amines in samples returned by
487   Stardust. Meteorit. Planet. Sci. 2008, **43**, 399-413.

488   (29) Elsila JE, Glavin DP, & Dworkin JP (2009) Cometary glycine detected in samples returned by Stardust.
489   Meteoritics and Planetary Science 44(9):1323-1330.

490   (30) Elsila J. E., Callahan M. P., Dworkin J. P., Glavin D. P., McLain H. L., Noble S. K., and Gibson Jr. E. K.
491   (2016b) The origin of amino acids in lunar regolith samples. Geomchim. Cosmochim. Acta **172**, 357-
492   369.

493   (31) Altwegg, K.; Balsiger, H.; Bar-Nun, A.; Berthelier, J.-J.; Bieler, A.; Bochsler, P.; Briois, C.; Calmonte,
494   U.; Combi, M. R.; Cottin, H.; De Keyser, J.; Dhooghe, F.; Fiethe, B.; Fuselier, S. A.; Gasc, S.; Gombosi,
495   T. I.; Hansen, K. C.; Haessig, M.; Jäckel, A.; Kopp, E.; Korth, A.; Le Roy, L.; Mall, U.; Marty, B.; Mousis,
496   O.; Owen, T.; Rème, H.; Rubin, M.; Sémon, T.; Tzou, C.-Y.; Waite, J. H.; Wurz, P. (2016) Prebiotic
497   chemicals -amino acid and phosphorus- in the coma of comet 67P/Churyumov-Gerasimenko. Sci.
498   Adv.**2**, e1600285.

499   (32) Cronin J. R. and Pizzarello S. 1997. Enantiomeric excesses in meteoritic amino acids. Science **275**,
500   951-955.

501   (33) Pizzarello S., Zolensky M. and Turk K. A. (2003) Nonracemic isovaline in the Murchison meteorite:
502   Chiral distribution and mineral association. Geochim. Cosmochim. Acta **67**, 1589-1595.

503   (34) Glavin D. P., Callahan M. P., Dworkin J. P., and Elsila J. E. (2010) The effects of parent body processes
504   on amino acids in carbonaceous chondrites. Meteorit. Planet. Sci. **45**, 1948-1972.

505   (35) Cox J. S., and Seward T. M. (2007) The reaction kinetics of alanine and glycine under hydrothermal
506   conditions. Geochim. Cosmochim. Acta, **71**, 2264-2284.

507   (36) Pietrucci F., and Saitta A. M. (2015) Formamide reaction network in gas phase and solution via a
508   unified theoretical approach: Toward a reconciliation of different prebiotic scenarios. Proceedings
509   of the National Academy of Sciences **112**, 15030-15035.

510 (37) Pietrucci F. (2017) Strategies for the exploration of free energy landscapes: Unity in diversity and
511   challenges ahead. Rev. Phys. **2**, 32-45.

512 (38) Pérez-Villa A., Georgelin T., Lambert J.F., Maurel M.C., Guyot F., Saitta A.M.,   Pietrucci   F.
513   (2017) A common precursor to both prebiotic and biological pathways to RNA nucleotides.
514   ChemRxiv DOI: 10.26434/chemrxiv.5519041.

515 (39) Saitta A. M. and Saija F. (2014) Miller experiments in atomistic computer simulations. Proceedings
516   of the National Academy of Sciences **111**, 13768-13773.

517 (40) Clayton R. N., and Mayeda T. K. (1999) Oxygen isotope studies of carbonaceous chondrites.
518   *Geochimica et Cosmochimica Acta* **63**, 2089-2104.

519 (41) Keil. Thermal alteration of asteroids: evidence from meteorites. Planet. Space Sci. 2000, 48, 887-
520   903.

521 (42) Brearley A. J. 2006. The action of water. In *Meteorites and the Early Solar System II* (eds. D. S.
522   Lauretta, L. A. Leshin and H. Y. McSween), pp. 587-624. University of Arizona Press: Tucson, AZ.

523 (43) Guo and Eiler. Temperatures of aqueous alteration and evidence for methane generation on the
524   parent bodies of the CM chondrites. Geochim. Cosmochim. Acta 2007, 71, 5565-5575.

525 (44) Pizzarello S., Williams L. B., Lehman J., Holland G. P. and Yarger J. L. (2011) Abundant ammonia in
526   primitive asteroids and the case for a possible exobiology. Proc. Natl. Acad. Sci. USA **108**, 4303-4306.

527 (45) Perdew J.P., Burke K., Ernzerhof M. (1996) Generalized gradient approximation made simple. Phys.
528   Rev. Lett. **77**, 3865-3868.

529 (46) Grimme S. (2006) Semiempirical gga-type density functional constructed with a long-range
530   dispersion correction. J. Comput. Chem. **27**, 1787-1799.

531 (47) CPMD Copyright IBM Corp. and by Max Planck Institute Stuttgart. www.cpmd.org, 2000-2017.

532 (48) Laio A., Parrinello M. (2002) Escaping free-energy minima. Proc. Natl. Acad. Sci.   U.S.A., **99**, 12562-
533   12566.

534 (49) Torrie G.M., Valleau J.P. (1977) Nonphysical sampling distributions in monte carlo free-energy
535   estimation: Umbrella sampling. J. Comput. Phys. **23**, 187-199.

536 (50) Bonomi M. et al. (2009) PLUMED: a portable plugin for free-energy calculations with molecular
537   dynamics. Comput. Phys. Commun. **180**, 1961-1972.

538 (51) Wang X., Conway W., Burns R., McCann N., Maeder M. (2010) Comprehensive Study of the
539   Hydration and Dehydration Reactions of Carbon Dioxide in Aqueous Solution. J. Phys. Chem. A **114**,
540   1734-1740.

541 (52) Buckles R.E., Mock G.V., Locatell L. (1955) Tiglic and angelic acids. Chem. Rev. **55**, 659-677.

542 (53) Alexandrova A. N. N., and Jorgensen W. L. (2011) On the mechanism and rate of spontaneous
543   decomposition of amino acids. J. Phys. Chem. B **115**, 13624-13632.

544 (54) Snider M. J., and Wolfenden R. (2000) The rate of spontaneous decarboxylation of amino acids. J.
545   Am. Chem. Soc. **122**, 11507–11508.

546 (55) Sato N., Quitain A. T., Kang K., Daimon H., and Fujie K. (2004) Reaction kinetics of amino acid
547   decomposition in high-temperature and high-pressure water. Ind. Eng. Chem. Res. **43**, 3217-3222.

548 (56) Li J., and Brill T. B. (2003) Spectroscopy of hydrothermal reactions. Int. J. Chem. Kinet. **35**, 602–610.

549 (57) Grimme S., Antony J., Ehrlich S., Krieg H. (2010) A consistent and accurate ab initio parametrization
550   of density functional dispersion correction (DFT-D) for the 94 elements H-Pu. J. Chem. Phys. **132**,
551   154104.

552 (58) Kuan, Y.-J.; Charnley, S. B.; Huang, H.-C.; Tseng, W.-L.; Kisiel, Z. (2003) Interstellar glycine. Astrophys.
553   J. **593**, 848-867.

554 (59) Snyder, L. E.; Lovas, F. J.; Hollis, J. M.; Friedel, D. N.; Jewell, P. R.; Remijan, A.; Ilyushin, V. V.; Alekseev,
555   E. A.; Dyubko, S. F. (2005) A rigorous attempt to verify interstellar glycine. Astrophys. J. **619**, 914-
556   930.

557 (60) Bernstein, M. P.; Dworkin, J. P.; Sandford, S. A.; Cooper, G. W.; Allamandola, L. J. Racemic amino
558   acids from the ultraviolet photolysis of interstellar ice analogues. Nature 2002, 416, 401-403.

559 (61) Muñoz-Caro, G. M.; Meierhenrich, U. J.; Schutte, W. A.; Barbier, B.; Segovia, A. A.; Rosenbauer, H.;
560   Thiemann, W. H.-P.; Brack, A.; Greenberg, J. M. Amino acids from ultraviolet irradiation of
561   interstellar ice analogues. Nature 2002, 416, 403-406.

562 (62) Danger, G.; Borget, F.; Chomat, M.; Duvernay, F.; Theulé, P.; Guillemin, J.-C.; d'Hendecourt, L. L. S.;
563   Chiavassa, T. Experimental investigation of aminoacetonitrile formation through the Strecker
564   synthesis in astrophysical-like conditions: Reactivity of methanimine (CH_2NH), ammonia (NH_3), and
565   hydrogen cyanide (HCN). Astron. Astrophys. 2011a, **535**, A47 (9pp).

566 (63) Yuen, G. U.; Kvenvolden K. A. (1973). Monocarboxylic acids in Murray and Murchison carbonaceous
567   chondrites. Nature **246**, 301-302.

568 (64) Hawkins J. M. and Fu G. C. (1986) Asymmetric Michael reactions of 3,5-dihydro-4H-dinaphth[2,1-
569   c:1',2'-e]azepine with methyl crotonate. J. Org. Che. **51**, 2820-2822.

570 (65) Pardo L., Osman R., Weinstein, Rabinowitz J. R. (1993) Mechanisms of Nucleophilic Addition to
571   Activated Double Bonds: 1,2- and 1,4-Michael Addition of Ammonia. J. Am. Chem. Soc. **115**, 8263-
572   8269.

573   (66)   Ehrenfreund, P.; Glavin, D. P.; Botta, O.; Cooper, G.; Bada, J. L. (2001) Extraterrestrial amino acids in
574   Orgueil and Ivuna: Tracing the parent body of CI type carbonaceous chondrites. Proc. Natl. Acad.
575   Sci. U.S.A. **98**, 2138-2141.

576   (67)   Aponte, J. C.; Abreu, N. M.; Dworkin, J. P.; Elsila, J. E. (2017) Distribution of Aliphatic Amines in CO,
577   CV and CK Carbonaceous Chondrites and Relation to Mineralogy and Processing History. Meteoritics
578   & Planetary Science **52**, 2632-2646.

579   (68)   S. Pizzarello, Y. Huang, and M. R. Alexandre (2008) Proceedings of the National Academy of Sciences
580   **105**, 3700-3704.

581   (69)   Pizzarello S. and Yarnes T. (2016) Enantiomeric excesses of chiral amines in ammonia-rich
582   carbonaceous meteorites. Earth Planet. Sci. Lett. **443**, 176-184.

583   (70)   Pollock G. E., Cheng C.-N., Cronin S. E., Kvenvolden K. A. (1975) Stereoisomers of isovaline in the
584   Murchison meteorite. Geochim. Cosmochim. Acta **39**, 1571-1573.

585   (71)   Soai K., Shibata T., Morioka H., and Choji K. 1995. Asymmetric autocatalysis and amplification of
586   enantiomeric excess of a chiral molecule. Nature **378**, 767–768.

587   (72)   Klussmann M., Iwamura H., Mathew S. P., Wells D. H., Pandya U., Armstrong A., and Blackmond D.
588   G. 2006. Thermodynamic control of asymmetric amplification in amino acid catalysis. Nature **441**,
589   621–623.

590   (73)   Savin, A., Nesper, R., Wengert, S. and Fässler, T. F. (1997) ELF: The Electron Localization Function.
591   Angew. Chem. Int. Ed. Engl. **36**, 1808–1832.

592   **Scheme 1.** Structures of glycine and isovaline zwitterions (color highlights the amine [blue, NH_2] and acid

593   [red, CO_2H] functional groups). Illustration of the different degree of steric hindrance around the alpha-
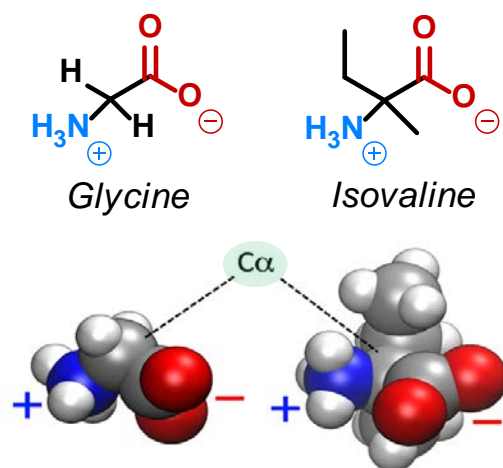
594   carbon (C_α).

595
596

597

Figure 1. Decomposition reactions of glycine (A) and isovaline (B) evaluated in this work. All simulations are performed in bulk water solution at T = 373 K. Reactions marked with an X never occur in our simulations: see the related discussion in the Results section. We equate (*S*)- to L-enantiomers for consistency to the nomenclature used in previous meteoritic amino acid studies.
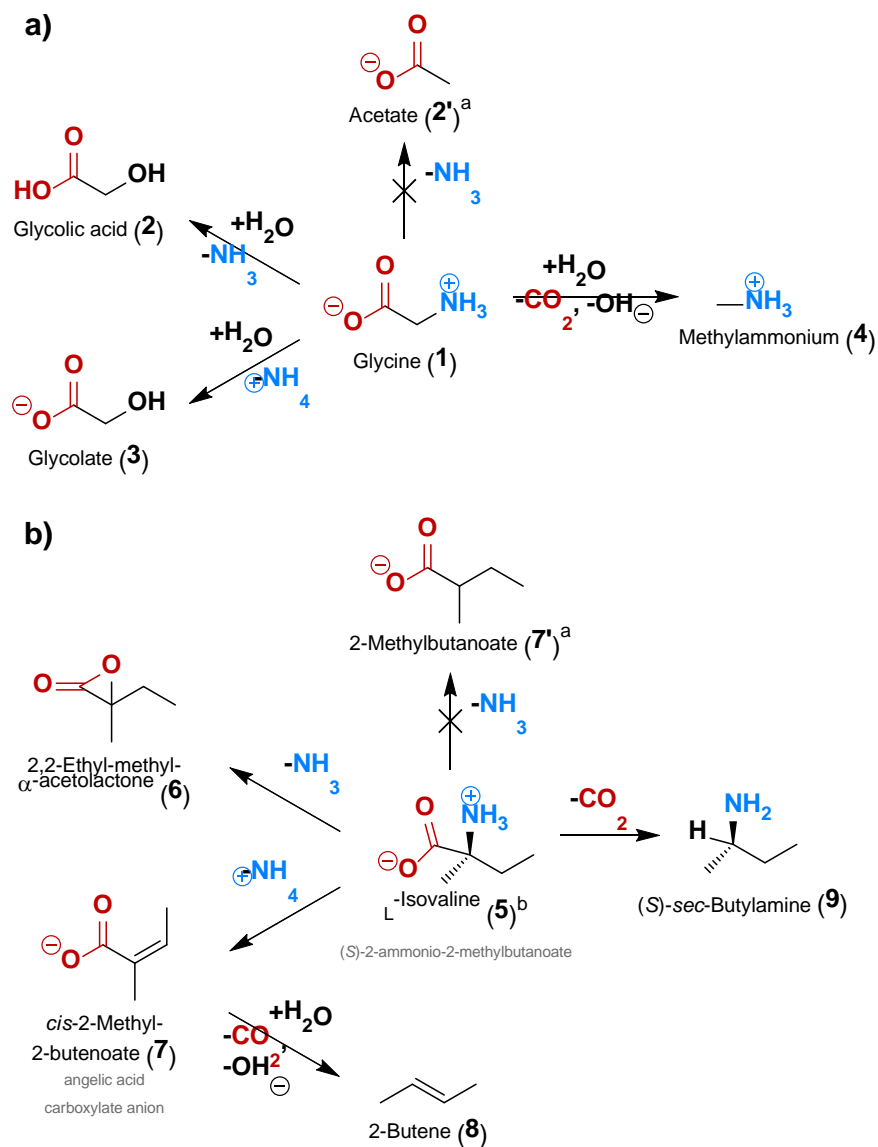

a)

Acetate (**2'**)[a]

Glycolic acid (**2**)

Glycolate (**3**)

Glycine (**1**)

Methylammonium (**4**)

b)

2-Methylbutanoate (**7'**)[a]

2,2-Ethyl-methyl-α-acetolactone (**6**)

L-Isovaline (**5**)[b]
(*S*)-2-ammonio-2-methylbutanoate

(*S*)-*sec*-Butylamine (**9**)

cis-2-Methyl-2-butenoate (**7**)
angelic acid carboxylate anion

2-Butene (**8**)

27

605 **Figure 2.** Schematic free-energy profiles of a) glycine and b) isovaline hydrothermal decomposition
606 processes from *ab initio* simulations. Statistical uncertainties are estimated as ±1 kcal/mol.
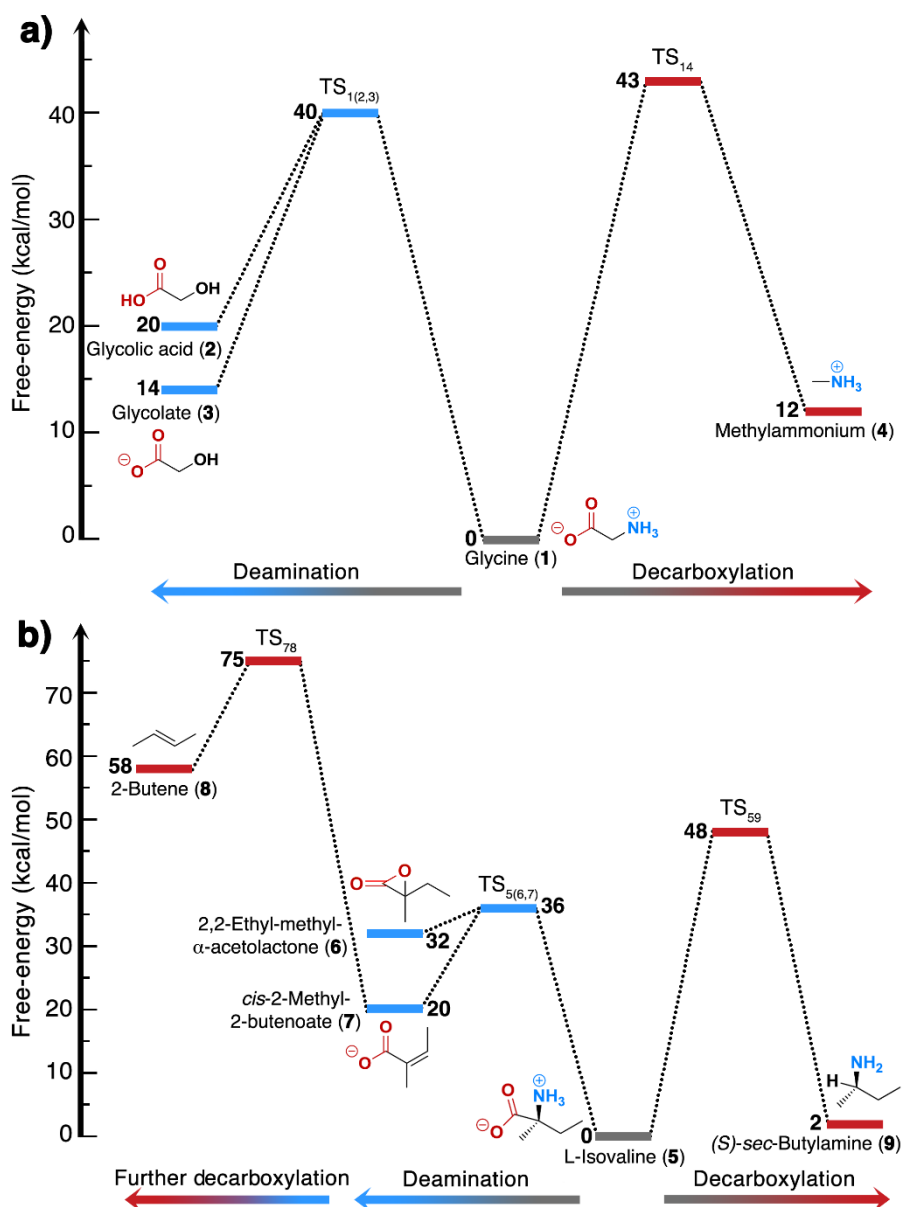
607

608
609

Figure 3. Free-energy landscapes of chemical reactions at *T*=373 K as a function of path collective

611   variables based on distances between atomic coordination patterns[36]. The landscapes are obtained from

612   weighted histogram analysis applied to *ab initio* umbrella sampling simulations, a) glycine deamination

613   to (**2**), b) glycine deamination to (**3**), c) glycine decarboxylation to (**4**), d) isovaline deamination to (**7**), e)

614   (**7**) decarboxylation to (**8**), and f) isovaline decarboxylation to (**9**).
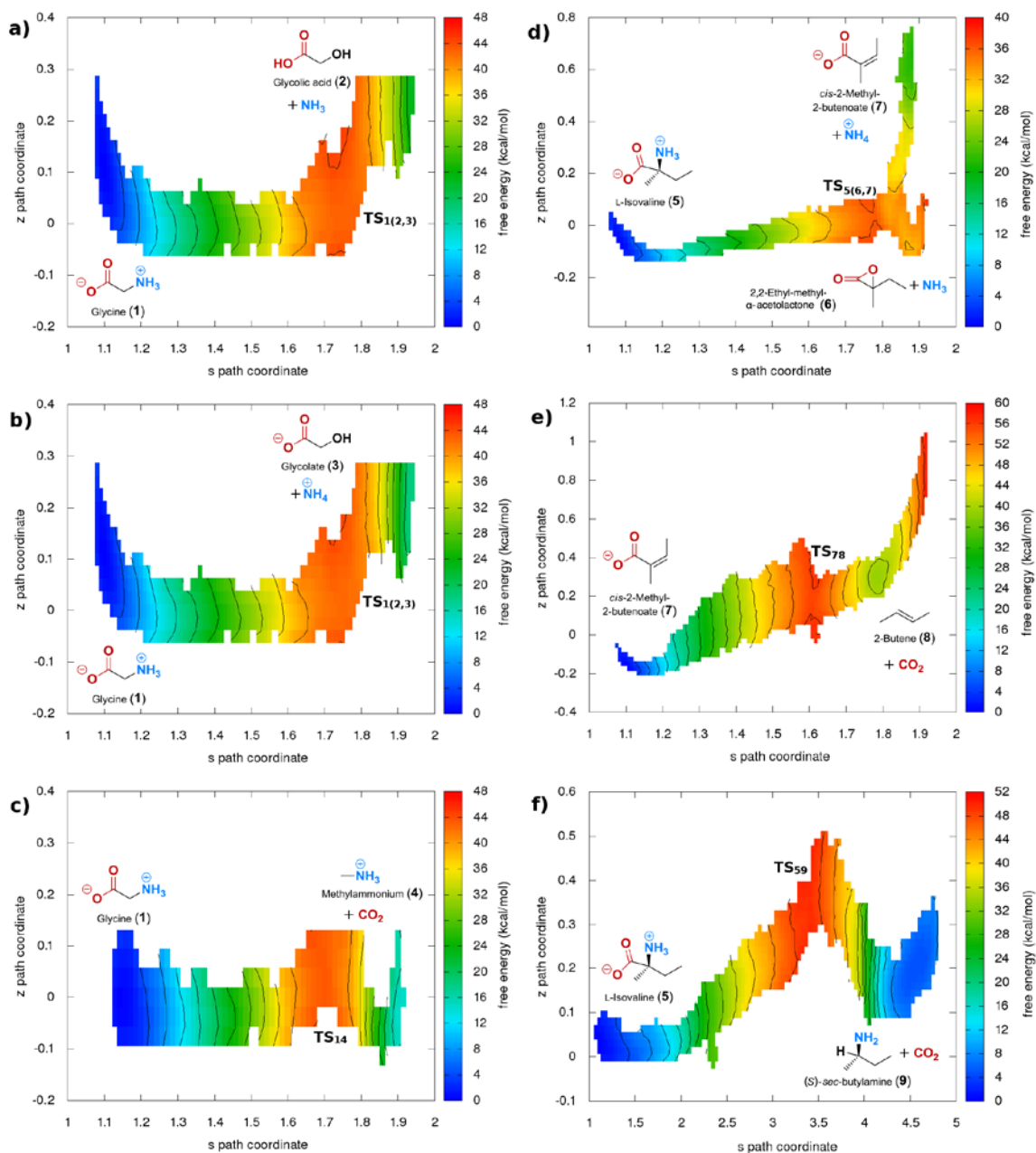
615

616

617   **Figure 4.** Representative transition state structures, identified by means of committor analysis on
618   umbrella sampling trajectories for a) glycine deamination, b) glycine decarboxylation, c) isovaline
619   deamination, d) angelic acid decarboxylation, and e) isovaline decarboxylation.
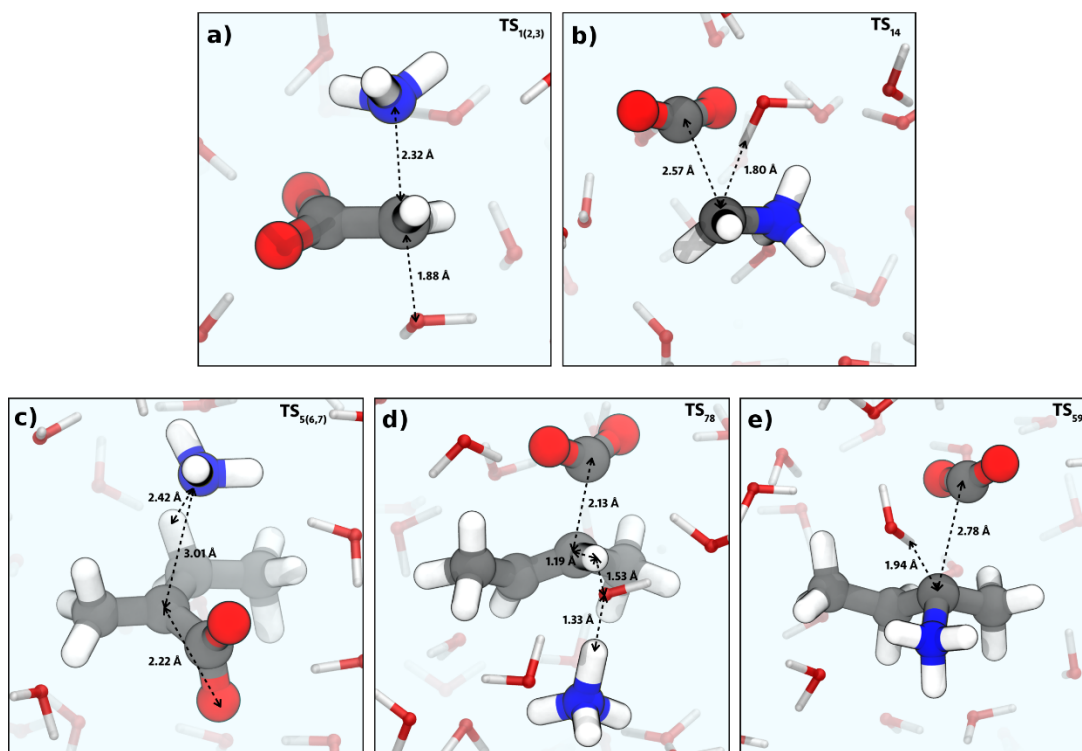
620

621

622 **Figure 5.** Electronic structure of the transition state configurations, represented by means of different
623 isovalues of the electron localization function.[73] Solvent water molecules are present in the calculations
624 but not depicted here, except for those undergoing bond breaking/formation. The corresponding
625 reactions are a) glycine deamination, b) glycine decarboxylation, c) isovaline deamination, d) angelic acid
626 decarboxylation, and e) isovaline decarboxylation. The carbocation character of the C_α is evident in panels
627 a) and c), whereas its carbanion character is evident in panels b) and e).

628

629